Available online at www.sciencedirect.com

SCIENCE DIRECT

Virology 332 (2005) 347–358

VIROLOGY

www.elsevier.com/locate/yviro

Role of HIV-2 envelope in Lv2-mediated restriction

Sandra Reuter, Patrick Kaumanns, Sabine B. Buschhorn, Matthias T. Dittmar*

Department of Virology, University of Heidelberg, Im Neuenheimer Feld 324, D-69120 Heidelberg, Germany

Received 24 August 2004; returned to author for revision 24 September 2004; accepted 18 November 2004
Available online 18 December 2004

Abstract

We have characterized envelope protein pseudotyped HIV-2 particles derived from two HIV-2 isolates termed prCBL23 and CBL23 in order to define the role of the envelope protein for the Lv2-mediated restriction to infection. Previously, it has been described that the primary isolate prCBL23 is restricted to infection of several human cell types, whereas the T cell line adapted isolate CBL23 is not restricted in these cell types. Molecular cloning of the two isolates revealed that the env and the gag gene are responsible for the observed phenotype and that this restriction is mediated by Lv2, which is distinct from Ref1/Lv1 (Schmitz, C., Marchant, D., Neil, S.J., Aubin, K., Reuter, S., Dittmar, M.T., McKnight, A., Kizhatil, K., Albritton, L.M., 2004. Lv2, a novel postentry restriction, is mediated by both capsid and envelope. J. Virol. 78 (4), 2006–2016).

We generated pseudotyped viruses consisting of HIV-2 (ROD-AΔenv-GFP, ROD-AΔenv-RFP, or ROD-AΔenv-REN) and the prCBL23 or CBL23 envelope proteins as well as chimeric proteins between these envelopes. We demonstrate that a single amino acid exchange at position 74 in the surface unit of CBL23-Env confers restriction to infection. This single point mutation causes tighter CD4 binding, resulting in a less efficient fusion into the cytosol of the restricted cell line. Prevention of endosome formation and prevention of endosome acidification enhance infectivity of the restricted particles for GHOST/X4 cells indicating a degradative lysosomal pathway as a cause for the reduced cytosolic entry. The described restriction to infection of the primary isolate prCBL23 is therefore largely caused by an entry defect. A remaining restriction to infection (19-fold) is preserved when endosomal acidification is prevented. This restriction to infection is also dependent on the presence of the point mutation at position 74 (G74E).

Keywords: Retroviral restriction; HIV-2; Lv2; Viral entry

Introduction

Early steps of the replication cycle of the human immunodeficiency virus have been at the center of attention since the discovery of the HIV co-receptors and the elucidation of the molecular basis of transmembrane protein mediated virus–cell fusion (Berger et al., 1999; Clapham and McKnight, 2002). The interaction of the surface unit of the viral envelope protein of HIV with CD4 and a chemokine receptor leads to the insertion of the fusion peptide into the target cell membrane. This peptide is part of the transmembrane protein of the viral envelope, which facilitates, through conserved helical structures (HR1 and HR2), the formation of a fusion pore to allow the viral core to enter the cytoplasm (for review, see Eckert and Kim, 2001). After exposure of the viral core inside the cell, only limited information is available about the processes resulting in successful integration of the proviral genome. Such post-entry events include the release of the viral RNA genome from the core, formation of the pre-integration complex (PIC), initiation of reverse transcription, and transport of the proviral genome to the nucleus.

Although these post-entry steps in the replication cycle have been biochemically defined, a clear understanding of these processes is only slowly emerging (for review, see Dvorin and Malim, 2003). Due to the apparent instability of the viral core, it is believed that this structure disassembles shortly after being released into the cytoplasm followed by the formation of the pre-integration complex. Whether the initiation of reverse transcription takes place inside the core

* Corresponding author. Fax: +49 6221 565003.
E-mail address: Matthias_Dittmar@med.uni-heidelberg.de (M.T. Dittmar).

0042-6822/$ - see front matter © 2004 Elsevier Inc. All rights reserved.
doi:10.1016/j.virol.2004.11.025

or during core disassembly is unknown. Apart from the viral RNA, reverse transcriptase, integrase, and several other viral and cellular proteins have been implicated to be part of this complex (Greene and Peterlin, 2002). Because of the high viscosity of the cytoplasm, movement of the PIC by diffusion is very limited. The microtuble network and dynein are implicated as the cellular structures that facilitate movement of the PIC towards the nucleus (McDonald et al., 2002).

A number of cellular host factors that interfere with early steps of the retroviral replication process have been identified. For example, actin microfilaments have been implicated in the formation of PIC (Bukrinskaya et al., 1998). Furthermore, the product of the murine Fv-1 gene, a derivative of an murine endogenous retroviral gag gene, limits the replication of certain murine leukemia virus strains (Best et al., 1996) in rodent cell lines and is therefore by definition a restriction factor. Human and monkey cell lines express a factor, called Ref1/Lv1, which restricts N-MLV and other retroviruses. Such restriction factors in primate cells target the viral capsid proteins prior to initiation or completion of the reverse transcription (Stoye, 2002; Towers et al., 2000).

Recently, Stremlau et al. (2004) characterized a member of the TRIM family as a restriction factor active in primate cells. Overexpression of TRIM5α in HeLa/CD4 cells results in substantial decrease of infection of HIV-1 when the TRIM5α variant from rhesus macaques was introduced. TRIM5α from African Green Monkeys constitutes a restriction factor as well (Hatziioannou et al., 2004; Keckesova et al., 2004; Perron et al., 2004; Yap et al., 2004). The human homologue showed only weak activity. Most of those studies to characterize Ref1/Lv1 and similar factors have been conducted using VSV-G envelope pseudotyped particles; therefore, Ref1/Lv1 restriction is independent of the route of viral entry. We have shown previously that Lv2, which is distinct from Ref1/Lv1, acts at earlier steps of the viral life cycle and is overcome with VSV-G pseudotyped HIV-2 isolates (McKnight et al., 2001; Schmitz et al., 2004).

The initial interaction of the viral envelope with the entry receptors or other surface structures primes the target cell to facilitate successful integration. Mori et al. (1993) observed that the envelope protein restricted the replication of a certain SIV strain in macrophages at a post entry step. Likewise, the infection of human macrophages by X4-tropic HIV-1 strains has been shown to be restricted at a post-entry level post-reverse transcription (Schmidtmayerova et al., 1998; Verani et al., 1998). Furthermore, a correlation between the capacity of a CCR5-tropic envelope protein to induce signals through CCR5 and the replication in macrophages has been described (Arthos et al., 2000). CCR5-tropic viruses activate MEK/ERK, as well as JNK and p38 MAPKs (Popik and Pitha, 2000a). Similarly, interaction of CXCR4 tropic isolates with CXCR4 on target cells activates the MEK/ERK pathway, at least for certain cell lines (Kinet et al., 2002). Ultimately, such signals may facilitate reverse transcription and integration, steps of the HIV replication cycle that are known to depend on the state of cell activation (Alfano et al., 1999, 2000; Arthos et al., 2000; Cicala et al., 1999; Liu et al., 2000) and may be linked to the inhibitory function of restriction factor(s).

Here, we analyzed the role of the envelope protein of a primary HIV-2 isolate for the restriction to infection of human cells. We demonstrate that a single amino acid exchange at position 74 in the surface unit of CBL23-Env confers restriction to infection. This single point mutation causes tighter CD4 binding resulting in a less efficient fusion into the cytosol of the restricted cell line. Prevention of endosome formation and prevention of endosome acidification enhance infectivity of the restricted particles for GHOST/X4 cells, indicating a degradative lysosomal pathway as a cause for the reduced cytosolic entry. The described restriction to infection of the primary isolate prCBL23 (McKnight et al., 2001; Schmitz et al., 2004) is therefore largely caused by an entry defect. However, a remaining restriction to infection (19 fold) is preserved when endosomal acidification is prevented. This restriction to infection is also dependent on the presence of the point mutation at position 74 (G74E) and could therefore, together with the capsid dependent restriction to infection, account for the LV2-mediated restriction in human cells.

Results

HIV-2 envelope pseudotyped HIV-2 particles confirm the envelope-dependent restriction to infection of GHOST-X4 cells

Molecular clones derived from the isolate prCBL23 encode for a premature stop codon in the envelope glycoprotein, resulting in a truncated cytoplasmic tail of the transmembrane protein gp35 compared to the full-length envelope of CBL23 (Schmitz et al., 2004). In order to compare the envelope genes of both virus isolates, HIV-2 reporter vectors were constructed, which do not express the envelope gene and contain a reporter gene (EGFP, mRFP, or renilla luciferase, respectively) instead of the HIV-2 *nef* gene (Fig. 1A). These reporter vectors were used to generate pseudotyped virus particles containing the envelope proteins of prCBL23 and CBL23 respectively. This was achieved after cloning recombinant envelope genes into the murine retroviral expression vector MP11 to obtain high levels of envelope protein production after co-transfection.

The first set of studied recombinant env-expression vectors (Fig. 1B) encoded the parental prCBL23 and CBL23 envelopes (Env35 and Env42) and a variant of prCBL23, in which the premature stop codon was mutated to the amino acid tryptophan (present in CBL23: Env35R2). Additionally, a truncated envelope of CBL23 with a stop codon at position 742 was constructed (Env42S).

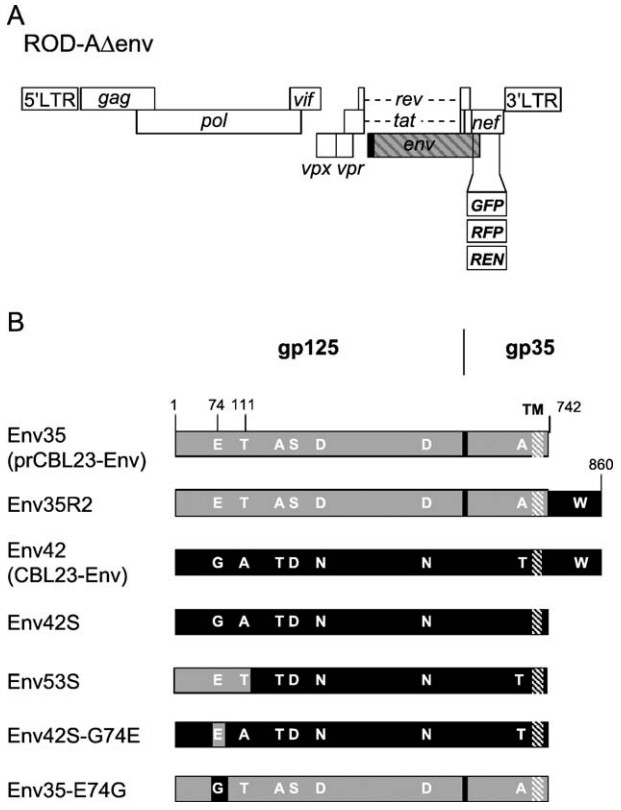

Fig. 1. Schematic representation of the envelope-minus reporter vectors and envelope proteins used to examine the role of the HIV-2 envelope in the Lv2-mediated restriction to infection. (A) The vector ROD-AΔenv was constructed using the ROD-A molecular clone ACR23 through deletion of the first eight amino acids of the *env* ORF (black bar). Fusion PCR was used to replace large parts of the nef open reading frame by the coding region of the green fluorescent protein, red fluorescent protein and renilla luciferase, resulting in ROD-AΔenv-GFP, ROD-AΔenv-RFP and ROD-AΔenv-REN, respectively. (B) Schematic representation of the envelope constructs used to define the region of the outer envelope responsible for the restriction to infection of GHOST/X4 cells. Shown are the two wild-type envelope proteins (prCBL23 = Env35 and CBL23 = Env42), the set of truncated or restored cytoplasmic tails of gp35 (Env35R2 and Env42S), and envelope proteins with point mutations at position 74 and 111 (Env53S) and position 74 only (Env42S-G74E, Env35-E74G). Bold letters indicate amino acid differences between the envelope proteins (gray = restricted; black = nonrestricted envelope proteins).

As described before, the ratio of infectious titres for the prCBL23 isolate on the two cell lines U87/CD4/X4 and GHOST/X4 shows a restriction to infection in comparison to CBL23. The isolate CBL23 is not restricted to infection in GHOST/X4 cells, and therefore the calculated ratio of infectious titres (U87/CD4/X4 vs. GHOST/X4) was set to 1 (McKnight et al., 2001; Schmitz et al., 2004). The pseudotyped HIV-2 particles, which had incorporated envelope proteins of prCBL23 (Env35, Env35R2) or CBL23 (Env42, Env42S), respectively, were used to infect both cell lines and the viral titres were determined. As Fig. 2 demonstrates, the infection of U87/CD4/X4 cells resulted in titres between 3×10^3 and 1×10^5 FFU/ml, depending on the HIV-2 pseudotype used (Fig. 2, left). The infection of GHOST/X4 cells resulted in infectious titres between 1×10^2 and 8×10^4 FFU/ml (Fig. 2, middle). The calculated ratio of infectious titres between both cell lines revealed that pseudotyped particles with incorporated Env35 displayed a 58-fold restriction to infection in comparison to the HIV-2[Env42] particles (Fig. 2, right panel). This 58-fold restriction was comparable to the fold restriction described before (McKnight et al., 2001; Schmitz et al., 2004). The truncation of the cytoplasmic tail in the CBL23 derived envelope (Env42S) did not result in a restriction to infection, whereas the restoration of a full-length cytoplasmic tail in the prCBL23 envelope (Env35R2) maintained the restriction, although at a reduced level (14-fold). Thus, envelope pseudotyped HIV-2 particles confirm the envelope-dependent restriction to infection and allow further analysis of the envelope region(s) responsible for this phenotype.

Since the truncation of the cytoplasmic tail does not cause a restriction to infection (HIV-2[Env42S]), we reasoned that a region in gp125, the surface unit (SU), is important for the restriction. To define precisely the envelope region(s) responsible for the restriction to infection of GHOST/X4 cells, several chimeric envelope expression plasmids were constructed and pseutotyped particles generated. Using the expression plasmid for

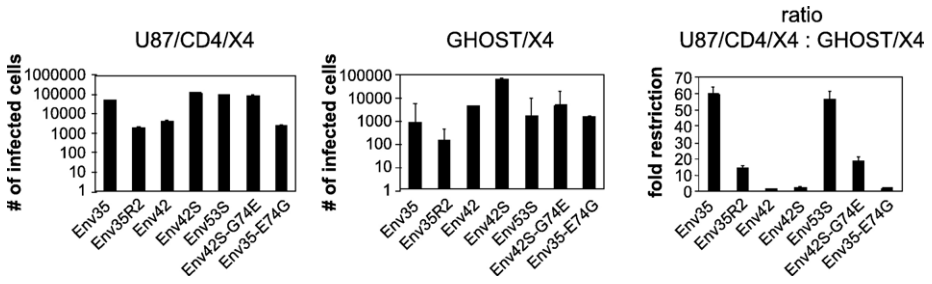

Fig. 2. Mapping the envelope molecular determinants responsible for the restriction to infection in GHOST/X4 cells. Equal volumes of pseudotyped particle stocks carrying the envelope proteins indicated were used to infect U87/CD4/X4 cells and GHOST/X4 cells. After 2 days, the cells were fixed, immunostained and the number of infected cells per infection was calculated (left and middle panel). Fold restriction refers to the infectious titres on U87/CD4/X4 cells compared to that on GHOST/X4 cells with error bars calculated from the results of three independent experiments (right panel). The ratio of infectious titres obtained from the infection with HIV-2[Env42] was arbitrarily set to 1 (for calculation, see Materials and methods and Schmitz et al., 2004).

Env42S, the 5′ end of gp125 coding region was exchanged and Env53S was generated. In addition, the amino acid at position 74 in Env42S was mutated to generate Env42S–G74E as well as the reverse mutation in the expression plasmid for Env35, resulting in Env35–E74G (Fig. 1B). These three chimeric envelope proteins were used to generate pseudotyped HIV-2 particles and the ratio of infectious titres for U87/CD4/X4 and GHOST/X4 was determined. Fig. 2 clearly indicates that the restriction to infection is conferred by the 5′ end of gp125. HIV-2[Env53S] particles showed a 55-fold restriction in comparison to HIV-2[Env42S] or HIV-2[Env42] particles. HIV-2[Env42S-G74E] particles showed a less pronounced but still substantial restriction to infection (20-fold). Pseudotyped particles with incorporated envelopes encoding the reverse mutation in the Env35 backbone, HIV-2[Env35-E74G], did not show the restriction to infection, as observed for the wild-type envelope Env35, thereby confirming the importance of amino acid 74 for the restriction. In addition, a mutation at position 111 in Env42S did not cause a restriction to infection and the reverse mutation in the prCBL23 envelope (Env35) did not abrogate the restriction to infection (data not shown).

HIV-2 entry route for GHOST/X4 cells differs between restricted and nonrestricted pseudotyped particles

Next, we determined the CD4 dependence of these pseudotyped particles using an anti-CD4 antibody to neutralize infection. Fig. 3A shows the inhibition of infection of the pseudotyped particles expressing different chimeric HIV-2 envelopes and HIV-2[VSV-G] particles. For these assays, the renilla luciferase encoding ROD-AΔenv-REN vector was used to generate pseudotyped particles. Infection in the absence of anti-CD4 antibody was set to 100% and relative infection in the presence of increasing concentrations of anti-CD4 antibody is depicted for both cell lines. This experiment showed that all viruses were equally well neutralized by anti-CD4 antibody when U87/CD4/X4 cells were used as target cells. However, the inhibition of infection by anti-CD4 antibody showed striking differences when GHOST/X4 cells were used. Only the nonrestricted particles HIV-2[Env42S] and HIV-2[Env35-E74G] were efficiently neutralized by anti-CD4 antibody. To reach a 50% inhibition of infection, a 4-fold higher concentration of anti-CD4 antibody was needed compared to U87/CD4/X4 cells, despite a lower steady state level of surface CD4 for GHOST/X4 cells as detected by FACS (data not shown). The restricted particles, carrying the envelopes Env35, Env53S, and Env42S-G74E, were 10-fold resistant to inhibition by anti-CD4 antibody compared to HIV-2[Env42S], indicating a stronger interaction of restricted envelope proteins with CD4 compared to the nonrestricted envelope protein Env42S. For both cell lines, the infection by HIV-2[VSV-G] was unaffected by the presence of anti-CD4 antibody.

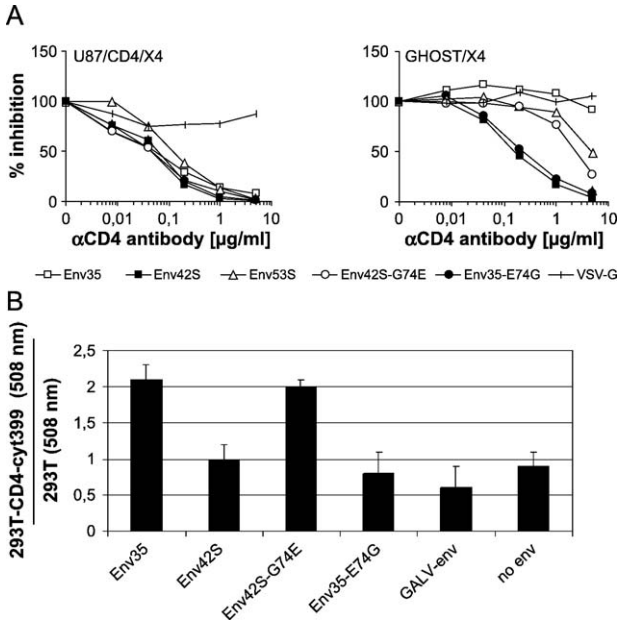

Fig. 3. Restricted pseudotyped particles display higher CD4 binding. (A) Sensitivity of pseudotyped HIV-2 particles to anti-CD4 antibody-mediated inhibition. U87/CD4/X4 and GHOST/X4 cells were pretreated for 30 min at 37 °C with anti-CD4 antibody at different concentrations (5, 1, 0.2, 0.04, and 0.002 µg of anti-CD4 antibody/ml) before adding equal amounts of pseudotyped particles (5 ng RT-equivalent). The cells were lysed at 2 days post-infection and the renilla luciferase activity (expressed due to infection with ROD-AΔenv-REN derived particles) was measured. Relative infection (% of control) was calculated by dividing the mean number of relative light units at each anti-CD4 antibody concentration by the mean number of relative light units from cells containing no antibody and is shown on the *y*-axis. The anti-CD4 antibody concentration is shown on the *x*-axis. Duplicate wells were analyzed for each drug concentration in at least three independent experiments. (B) Transiently transfected 293T cells expressing no CD4 or truncated CD4 (CD4-cyt399) were incubated with pseudotyped particles containing a mRFP-vpr2 fusion protein and the envelope proteins indicated. After incubation of particles with 293T cells (1 h at 37 °C), nonbound particles were removed and bound particles quantitated by detection of particle associated red fluorescence at 508 nm. As controls, envelope-deficient particles and particles pseudotyped with the envelope protein of GALV were used. The higher the fluorescence ratio (dividing the fluorescence obtained from 293T-CD4-cyt399 cells by the fluorescence obtained from mock transfected 293T cells), the stronger the CD4-dependent binding. Data are representative of results obtained in two independent experiments.

In order to address the envelope-CD4 binding in another system, we transiently transfected 293T cells with an expression plasmid encoding for a cytoplasmic tail truncated CD4 molecule. Tail-truncated CD4 (CD4-cyt399) is not endocytosed and remains at the cell surface, but supports HIV entry in the presence of the appropriate coreceptor (Bedinger et al., 1988; Maddon et al., 1988; Pelchen-Matthews et al., 1995). Incubation of mock-transfected or CD4-cyt399-transfected 293T cells with equal amounts of pseudotyped particles containing the mRFP-vpr2 fusion protein results in binding of particles to 293T cells dependent on the presence of CD4 alone. Quantitation of particle binding is possible due to the particle associated mRFP-vpr2 fusion proteins using a microplate fluorometer. As Fig. 3B

shows, the control particles containing no envelope protein or the envelope protein of Gibbon Ape Leukemia Virus (GALV) do not specifically bind to CD4-cyt399 (fluorescence ratio for 293T-CD4cyt399 cells vs. 293T cells around or below 1). The two restricted particles, HIV-2[Env35] and HIV-2[Env42-G74E], however, display a stronger CD4 binding capacity when compared to the nonrestricted particles HIV-2[Env42S] and HIV-2[Env35-E74G]. This result supports the initial notion that restricted particles bind tighter to CD4 than nonrestricted particles.

Next, we determined the virus–cell fusion efficiency of the restricted and nonrestricted particles. We made use of the recently described virion-based fusion assay (Cavrois et al., 2002; Lineberger et al., 2002) that measures cytosolic delivery of β-lactamase (BlaM) from virions into target cells. This assay has been shown to discriminate between fusion and endocytosis of virions due to the lack of CCF2/AM availability within endosomes (Cavrois et al., 2002; Schaeffer et al., 2004). Pseudotyped particles, which incorporated a fusion protein of BlaM::vpr2 were generated and used to infect U87/CD4/X4 and GHOST/X4 cells. Equal multiplicity of infection were used and after 3 h the cells were loaded with CCF2/AM for 18 h at room temperature. The fluorescence was measured in a microplate fluorometer. Fluorescence ratios were calculated after subtraction of background fluorescence of control cultures containing no virus. The results of triplicate values for both cell types are depicted in Fig. 4. As expected, the infection with envelope minus particles did not result in increasing fluorescence at 447 nm for either cell line. The infection of U87/CD4/X4 cells showed no significant differences between restricted and nonrestricted HIV-2 particles, although HIV-2[Env35R2] infection of U87/CD4/X4 cells resulted repeatedly in a lower fluorescence ratio. The infection of GHOST/X4 with the nonrestricted pseudotyped particles HIV-2[Env42] and HIV-2[Env42S] resulted in a significantly higher fluorescence at 447 nm when compared to the restricted pseudotyped particles, indicating a higher efficiency in reaching the cytoplasm. To analyze the fold restriction to fusion, we divided the fluorescence ratio obtained from the BlaM-assay for U87/CD4/X4 cells by the fluorescence ratio obtained from the BlaM-assay for GHOST/X4 cells. Fig. 4 (right panel) illustrates that the restricted envelope proteins Env35, Env53S, and Env42-G74E were 2.5- to 3-fold less efficient for virus entry when compared to the nonrestricted envelope proteins Env42, Env42S, and Env35E74G.

We hypothesized that the determined strong CD4 interaction and reduced viral entry could be reconciled by differences in endosomal uptake of bound particles by GHOST/X4 cells and subsequent degradation in lysosomes. Therefore, we determined the basal endocytosis rate of CD4 for U87/CD4/X4 cells and GHOST/X4 cells. Fig. 5A shows the result of the kinetic endocytosis assay performed. CD4 internalization from the cell surface does not differ between the two cell lines. After 40 min, 48% (U87/CD4/X4 cells) and 53% (GHOST/X4 cells) of the marked CD4 molecules remain at the cell surface. Since this assay does not measure a potential virus-induced CD4 internalization, we next studied the infectivity of restricted and nonrestricted particles depending on the presence of ammonium chloride (NH_4Cl), a lysomotropic weak base that prevents endosome and lysosome acidification. As has been described earlier, pre-incubation of target cells with NH_4Cl enhances HIV-1 infectivity in HeLa cells (Aiken, 1997). U87/CD4/X4 cells and GHOST/X4 cells were pre-incubated with NH_4Cl and subsequently infected using the pseudotyped particles HIV-2[Env35] and HIV-2[Env42S]. As Fig. 5B shows, the concentration of NH_4Cl used (10 mM) was sufficient to abrogate VSV-G mediated infection. Again, the direct comparison of restricted and nonrestricted particles revealed differences for the GHOST/X4 cells and not for U87/CD4/X4 cells. Pre-treatment with NH_4Cl caused a 10-fold increase of infectivity of the restricted HIV-2[Env35], and only a modest 1.4-fold increase for the nonrestricted HIV-2[Env42]. The infectivity on U87/CD4/X4 cells was less dependent on the NH_4Cl treatment for both pseudotyped particles, 1.9- and 0.8-fold, respectively.

In order to test endosomal uptake more directly, GHOST/X4 cells were transfected with dynamin and dynaminK44A expression plasmids. Both proteins were expressed as GFP-fusion proteins allowing quantification of the transfection

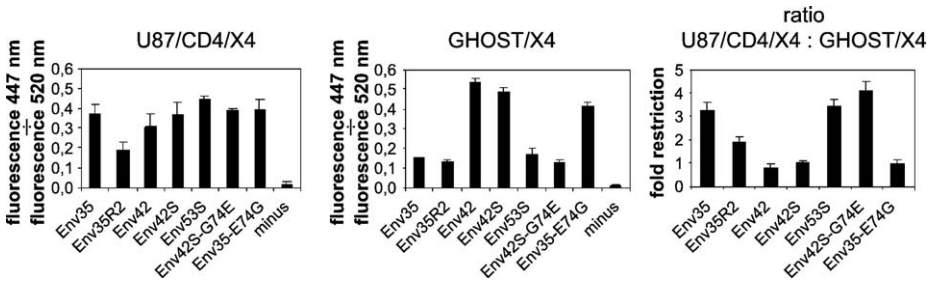

Fig. 4. Virus to cell fusion assay confirms reduced cytosolic entry for restricted particles. Restricted pseudotyped particles (Env35, Env35R2, Env53S, Env42S-G74E) and nonrestricted particles (Env42, Env42S) were assayed for fusion with U87/CD4/X4 cells (left) and GHOST/X4 cells (middle) in the BlaM-Vpr2 reporter assay. Data shown are mean of triplicate determinations and are representative of at least three independent experiments. Envelope-negative particles were used as negative controls. The fluorescence ratio (447 vs. 520 nm) is shown on the *y*-axis. Fold restriction of fusion into the cytoplasm was determined by dividing these fluorescence ratios obtained from U87/CD4/X4 cells and GHOST/X4 cells (right panel).

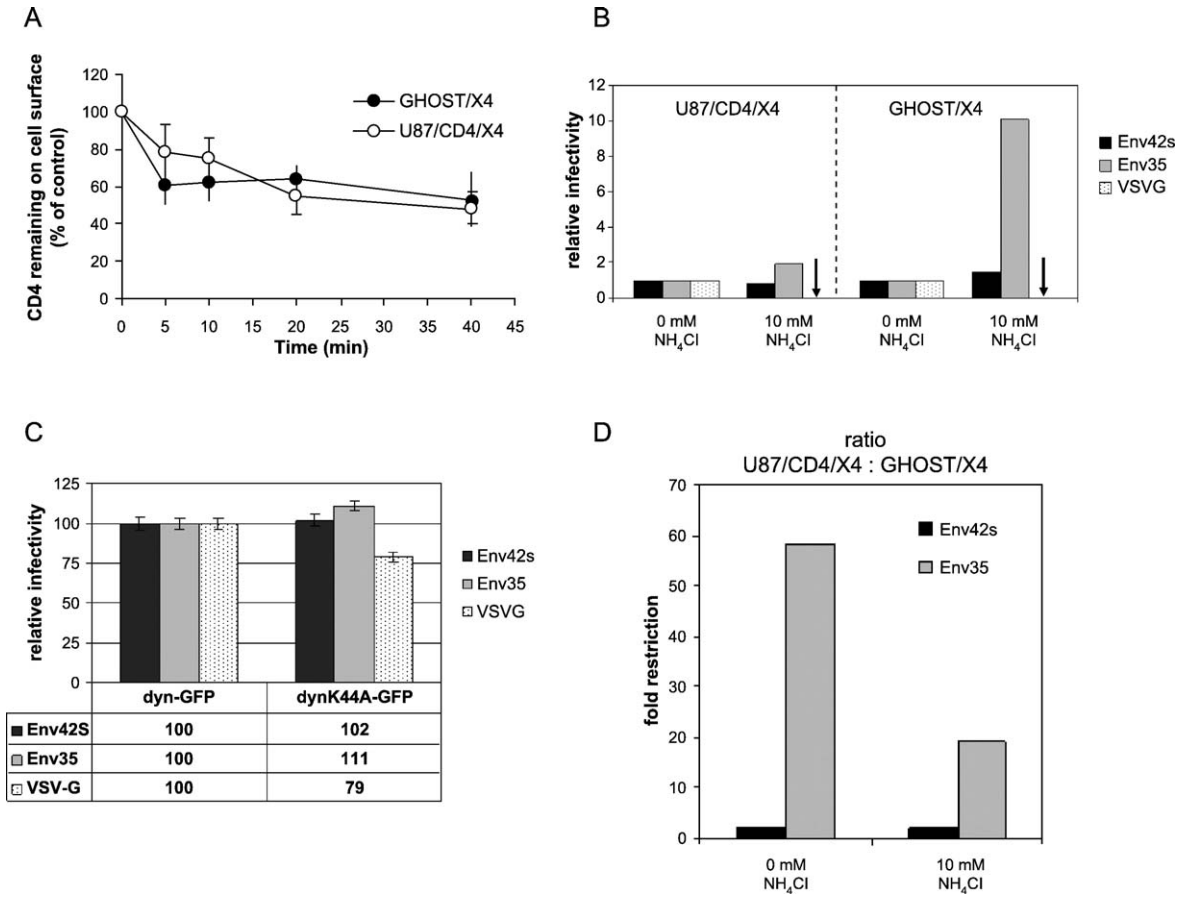

Fig. 5. Basal endocytosis of CD4 and endosomal uptake of particles. (A) Rate of CD4 endocytosis was analyzed for U87/CD4/X4 cells and GHOST/X4 cells over time. CD4 internalization from the cell surface is equally efficient for both cell lines. (B) Inhibition of endosomal acidification: For the inhibition of endosomal acidification, both cell lines were pretreated with NH_4Cl (10 mM) for 30 min at 37 °C before adding equal amounts of infectious virus (ROD-AΔenv-derived particles). The cells were immunostained 2 days post-infection and the number of blue cells determined. HIV-2[VSV-G] particles were used to control for complete inhibition of acidification of endosomes. (C) Relative infectivity of ROD-AΔenvRFP-derived particles after challenge of dynamin or dynaminK44A transfected GHOST/X4 cells. Forty-eight hours post-infection, red fluorescence at 607 nm and green fluorescence at 508 nm were determined. The ratio of red fluorescence versus green fluorescence allows the quantification of infectivity of the respective pseudotyped particles dependent on the expression of the GFP-dynamin fusion proteins. One representative experiment out of three is shown. (D) Fold restriction was determined by dividing the infectious titres obtained from U87/CD4/X4 cells and GHOST/X4 cells (results from experiment B) in the absence of NH_4Cl and in the presence of 10 mM NH_4Cl, respectively.

efficiency. Dominant-negative dynamin (dynK44A) has been shown to abrogate endosome formation (van der Bliek et al., 1993). Therefore, after challenge with HIV-2[Env35] pseudotyped particles, we expected an increase in infectivity and a decrease in infectivity for HIV-2[VSV-G] pseudotyped particles. Transiently transfected GHOST/X4 cells were seeded into 48-well trays and subsequently infected using ROD-AΔenvRFP derived pseudotyped particles HIV-2[Env35], HIV-2[Env42S], and HIV-2[VSV-G], respectively. Forty-eight hours post-infection, the total red fluorescence (infected cells) and green fluorescence (transfected cells) was determined. The transfection resulted in only 25% dynamin-expressing GHOST/X4 cells (data not shown). As Fig. 5C shows, this low transfection efficiency resulted nevertheless in a modest increase in infectivity for HIV-2[Env35] particles (11%) and a modest decrease in infectivity of HIV-2[VSV-G] particles (21%), supporting our hypothesis of endosomal uptake.

However, even after blocking endosomal acidification (Fig. 5B), a 19-fold restriction to infection in GHOST/X4 cells was observed (Fig. 5D). Since endosomal uptake has been shown to circumvent Lv2-mediated restriction (McKnight et al., 2001), the remaining restriction to infection could be a result of divergent entry pathways from distinct plasma membrane structures as initially proposed.

Stimulation of MAPK after particle binding

Since it has been shown that envelope–receptor interaction can result in the induction of the MAPK cascade (Popik and Pitha, 2000a), we also tested whether the restricted and nonrestricted envelope proteins of HIV-2 induce different intracellular signals upon binding to GHOST/X4 cells, thereby accounting for enhanced CD4 endocytosis. Serum-depleted cells were incubated with

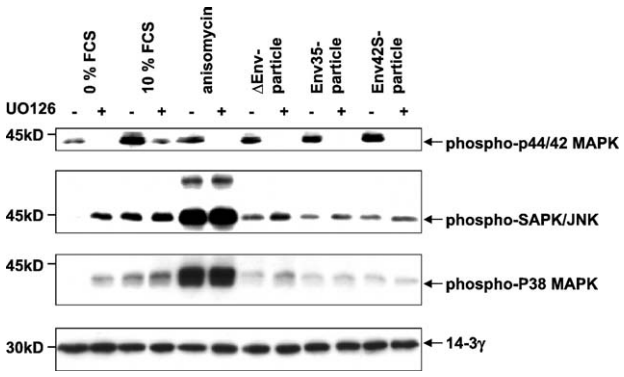

Fig. 6. Stimulation of p44/p42 MAPK by restricted and nonrestricted pseudotyped particles is equally efficient. GHOST/X4 cells were incubated with particle preparations (100 ng RT equivalents) carrying no envelope, Env35, Env42S, 200 ng/ml anisomycin or 10% FCS in the presence or absence of 50 μM UO126 for 30 min at 37 °C. Detection of p44/p42 MAPK, SAPK/JNK, and p38-MAPK was performed using the phospho-MAPK family antibody sampler kit. Blots were reprobed with anti-14-3-3γ to assure equivalent loading in each lane. Data are representative of results obtained in two independent experiments.

different particle preparations (no envelope, HIV-2[Env35], HIV-2[Env42S]) as well as 10% FCS or anisomycin, an activator for all three MAPK family members studied. Serum depletion resulted in a complete reduction of ppSAPK/JNK and pp38 MAPK, whereas some pp44/pp42 MAPK remained detectable. The MEK1/2 inhibitor UO126 was used to specifically block the activation of ERK1/2. After 30-min incubation with the different particles, the cells were lysed and immunoblotted. As Fig. 6 shows, the incubation of GHOST/X4 cells with a high concentration of FCS (10%) and with anisomycin (200 ng/ml) resulted in a substantial increase of activated p44/p42 MAPK. The incubation with UO126 inhibited this activation effectively. The incubation of GHOST/X4 cells with envelope-minus particles or particles carrying the restricted (Env35) or nonrestricted (Env42S) envelope proteins stimulated p44/p42 MAPK equally efficient and this stimulation was also blocked by UO126. For SAPK/JNK and p38-MAPK, stimulation was detected due to incubation with anisomycin (and was not blocked by UO126) but not due to incubation with pseudotyped particles. An ELISA-based quantitative analysis of ERK1/2 activity confirmed the results of the western blot analysis (data not shown). Therefore, a differential stimulation of MAPK family members cannot explain the differences in viral uptake observed for the HIV-2[Env35] pseudotyped particles.

Discussion

This study localizes a critical region in the envelope protein of the isolate prCBL23 that can alter entry events in the viral life cycle and refines a previously described restriction to infection of human cells by this HIV-2 isolate (McKnight et al., 2001; Schmitz et al., 2004). We employed a HIV-2ROD-derived, envelope gene deleted vector as backbone pseudotyped with envelope proteins derived from CBL23 and prCBL23. This has allowed us to study the role of the envelope proteins of CBL23 and prCBL23 independently of potential interactions of the capsid protein also shown to mediate post-entry restrictions (Schmitz et al., 2004). After analyzing a large set of chimeric envelope proteins, including single point mutations, we can conclude from the immunostaining experiments (Fig. 2) that the amino acid at position 74 (N-terminal of the V1 region) is responsible for the restriction to infection of GHOST/X4 cells.

It has been shown that receptor cell surface density is involved in infectivity of macrophages, thymocytes, and cell lines (Naif et al., 1998; Pedroza-Martins et al., 1998; Platt et al., 1998) and that certain envelope proteins have higher affinities to the corresponding receptors (for review, see Clapham and McKnight, 2002). We have performed assays to address the CD4 dependence of the restricted and nonrestricted envelope proteins. The amino acid exchange at position 74 does not result in CD4-independence, since for all chimeric envelope proteins studied, the IC_{50} values obtained from the inhibition of U87/CD4/X4 infection are comparable. Although GHOST/X4 cells display lower steady state levels of CD4 on their cell surface, larger amounts of anti-CD4 antibody was required to inhibit infection compared to U87/CD4/X4 cells. Moreover, despite the high concentration of anti-CD4 antibody used, the restricted particles carrying the envelope proteins Env35, Env53S, Env42S–G74E were not inhibited on GHOST/X4 cells, indicating a tighter gp125–CD4 interaction. This interpretation is supported by a particle binding assay (Fig. 3B) using transiently transfected 293T cells expressing cytoplasmic tail deleted CD4.

The results of the virus–cell fusion assay revealed that restricted particles are less efficient in fusion into the cytosol, since only the delivery of active BlaM into the cytosol results in cleavage of the fluorescent dye CCF2/AM (Fig. 4). Prevention of endosomal acidification resulted in enhanced infectivity for all pseudotyped particles examined, and this was more pronounced for the restricted particles carrying envelope protein Env35 (Fig. 5B). It has been shown that NH_4Cl treatment enhances entry via the fusion pathway for HIV-1 (Pelchen-Matthews et al., 1995; Schaeffer et al., 2004). Our studies confirm and extend this finding also reported by others (Fackler and Peterlin, 2000; Marechal et al., 2001) now including HIV-2. Moreover, transiently expressed dominant-negative dynamin (dynK44A) causes an increase in infectivity for HIV-2[Env35] on GHOST/X4 cells as well (Fig. 5C). These results together argue for enhanced endocytosis and degradation of restricted particles, which encode for glutamic acid at position 74 of the envelope protein. As has been shown before, single point mutations in the outer surface unit of the HIV-1 and SIV envelope proteins result in differences in viral infectivity and CD4 dependence (Otto et

al., 2003) although these differences were correlated to changes in the C3 region of the envelope protein. In addition, coreceptor binding is modulated by single mutations in the V3 loop and V1 loop, resulting for example in the infection of target cells expressing low CCR5 (Boyd et al., 1993; Clapham and McKnight, 2002; Dejucq et al., 1999; Reeves et al., 2004). A correlation between CD4 binding capacity, due to a mutation(s) upstream of the V1 loop of HIV-2 gp125, and viral uptake has not been described previously.

As has been described earlier, the ERK MAPK pathway regulates infectivity of HIV-1 (Yang and Gabuzda, 1999) and this pathway as well as the SAPK/JNK and p38-MAPK pathways can by induced by HIV-1 gp120 binding to target cells (Kinet et al., 2002; Popik and Pitha, 2000b) and play a role in entry and post-entry events (Chackerian et al., 1997). Therefore, we determined whether binding of particles to target cells cause activation of different signalling cascades, which could result in activation or inactivation of restriction factors leading to the restriction observed or bypassing the restriction observed, respectively. The activation of ERK, SAPK/JNK, or p38-MAPK signalling cascades, however, did not differ after binding of restricted envelope proteins compared to nonrestricted envelopes to GHOST/X4 cells (Fig. 6). Recently, it has been described that actin cytoskeleton rearrangement is important for virus-induced cell fusion and dependent on coreceptor-mediated activation of Rac, a downstream effector of Pyk2 (Pontow et al., 2004). Whether the activation of other protein kinases, like Pyk2, differ due to binding of restricted particles compared to nonrestricted particles remains to be shown.

With regard to the observed restriction to infection of GHOST/X4 cells, we demonstrate that a large part of this restriction is a direct consequence of tight CD4-binding and subsequent endosomal uptake, perhaps leading to degradation of particles in the lysosome, and not a post-entry restriction. However, even in the presence of 10 mM NH_4Cl, when endosomal acidification is blocked completely, we observe a remaining restriction to infection (19 fold) for particles carrying the restricted envelope protein Env35 compared to particles carrying the nonrestricted envelope protein Env42S (Fig. 5D). These results are in agreement with our previous finding using molecular clones of the two isolated prCBL23 and CBL23 (Schmitz et al., 2004), where the exchange of the entire envelope coding region of the restricted clone MCR by the envelope coding region of the nonrestricted clone MCN resulted in the reduction but not abrogation of the restriction to infection. Therefore, it is feasible that divergent entry pathways from distinct plasma membrane structures are used by HIV-2[Env35] in comparison to HIV-2[Env42S], as initially proposed (McKnight et al., 2001; Schmitz et al., 2004). Such divergent entry pathways could result in the delivery of the viral cores to different cytosolic compartments where the concentration and/or activity of restriction factors, like Lv2, differ. In addition, nuclear targeting of retroviral structures inside the cell is dependent of intact cytoskeleton (Kizhatil and Albritton, 1997; McDonald et al., 2002; Pontow et al., 2004). Therefore, differences in microtubules or actin-dependent movement could be the cause for the observed restriction to infection. New methods to follow the fate of retroviral structures in infected cells have been used successfully (McDonald et al., 2002) and future studies will address the localization of such structures inside the cell and potential differences between restricted and nonrestricted infection, thereby defining the postulated permissive cytosolic compartments. The existence of such permissive and nonpermissive cytosolic compartments, which have or have not access to the nucleus and bypass or overcome the action of restriction factors, needs to be addressed in the future.

In conclusion, we can show that a single point mutation (G74E) in the restricted envelope protein Env35 causes tighter CD4 binding on GHOST/X4 cells and enhanced endocytosis resulting in a less efficient fusion into the cytosol. The previously described restriction to infection of the primary isolate prCBL23 (McKnight et al., 2001; Schmitz et al., 2004) is therefore largely caused by an entry defect. However, a remaining restriction to infection (19-fold) is preserved when endosomal acidification is prevented. This restriction to infection is also dependent on the presence of the point mutation at position 74 (G74E) and could, therefore, together with the capsid-dependent restriction to infection, account for the Lv2-mediated restriction in human cells. More studies are needed to address this Lv2-dependent entry restriction.

Materials and methods

Cells and pseudotyped viruses

U87/CD4 cells expressing the chemokine receptor CXCR4 and GHOST-CXCR4 were provided by the EU programme EVA/MRC centralized facility for AIDS reagents, NIBSC, UK. HEK293T cells were used for transfection with ROD-AΔenv vectors and MP11-derived env-expression plasmids using Fugene6 (Roche, Germany). Virus containing supernatants were harvested 3 days later, filtered, and stored at −80 °C. Virus production into the supernatant was quantified by measurement of RT activity using a sensitive nonradioactive method (Retrosys RT activity kit, Cavidi Tech, Uppsala, Sweden).

Construction of ROD-AΔenv vectors and envelope expression plasmids

The vector ROD-AΔenv was constructed using the ROD-A molecular clone ACR23 as follows: The first eight nucleotides of the env ORF have been deleted by

site-directed mutagenesis PCR with the oligomers EnvΔ8 (5′-CCGTCGTCTCC TACACCAGACAAGTGAGTT-CAGCTGCTTATTGCC-3′) and ROD-A8581- (5′-GCGG-CCTGGAATGCTTCTTGGATC-3′). The resulting PCR fragment has been cloned into ACR23 via Esp3 (6129) and *Bsm*I (8581) to substitute the original sequence (numbering according to published ROD-A sequence).

Recombinant PCR was also used to replace large parts of the nef ORF by the coding region of the green fluorescent protein (EGFP, Clonetech, Germany), monomeric RFP (Campbell et al., 2002) and renilla luciferase, resulting in ROD-AΔenv-GFP, ROD-AΔenv-RFP and ROD-AΔenv-REN, respectively. For ROD-AΔenv-GFP, the primers rod7969+ (5′-TACTGTACCATGGGTTAATGATTCCTT-AGC-3′), rod/gpf− (5′-ATTGCAAGAAGGCTGTTCTAA-GTCTCA-3′), rod/gfp+ (5′-GACTTAGAACAGCCTTCTT-GCAATATGGTGAGCAAGGGCGAGGAGCTGTTC-3′), and gfp− (5′-TATATGCC ATGGTGATCAGTTATCTAG-ATCCGGTGGATC-3′) were used to perform a recombinant PCR. The corresponding *Nco*I–*Nco*I fragment of ACR23 was replaced by the fusion-PCR product encoding for EGFP instead of NEF. Similarly, the mRFP and renilla luciferase marker genes were introduced using specific primers to yield ROD-AΔenv-RFP and ROD-AΔenv-REN.

To amplify the envelope sequences of prCBL23 and CBL23 from molecular clones of these isolates, the following primer pairs were used: 5′-GGATA AGTCGC-GGCCGCATGATGGGTGGTAGAAATCAGCTGC-3′ and 5′-GCCAGGGAA GCTTTCATAGGAGGGCGATCTCTG-CTCCC-3′ creating a *Not*I site at the 5′end and a *Hin*dIII site at the 3′end. The PCR products were cloned into the expression vector pMP11 (Schambach et al., 2000) to create the plasmids Env35 and Env42. Env35R2 and Env42S were constructed by exchanging the 3′ ends of Env35 and Env42 via *Bst*EII (2129) and *Hin*dIII (MCS of MP11) (numbering according to the env-expression plasmid). The chimeric envelope Env53S was created by exchanging the very N-terminal part between Env35 and Env42S as indicated in Fig. 1B using the restriction sites *Not*I (located within the MP11 vector) and *Eco*RI (421). Single point mutation Envs (Env42S–G74E,and Env35–E74G) were created by fusion PCR thereby producing the exchanges G74E and E74G in Env42S or Env35, respectively.

Immunostaining of HIV-2-infected cells and calculation of restriction

The immunostaining method has been described before (McKnight et al., 2001). Briefly, HIV-infected cells were washed in serum-free phosphate-buffered saline (PBS) and fixed in methanol/acetone, 1:1 at −20 °C. After washing in PBS/1% FCS (PBS/FCS), HIV-2-positive serum was added at 1/5000 (in PBS/FCS) to detect virus antigen. After three washes in PBS/FCS, the cells were incubated for 1 h with mouse anti-human IgG conjugated with β-galactosidase (Southern Biotech). After a further three washes in serum-free PBS, 0.5 mg/ml X-gal substrate (Sigma, Germany) in PBS containing 3 mM potassium ferricyanide, 3 mM potassium ferrocyanide, and 1 mM magnesium chloride was added. Clusters of blue cells were counted as foci of infection (FFU) to estimate the viral titre. The restriction (*n*-fold) is calculated as the ratio of infectivity of unrestricted cells to restricted cells (ratio U87/CD/X4 vs. GHOST/X4 cells).

Viral entry assay

HIV-2 particles carrying a β-lactamase reporter protein were produced by cotransfection of 293T cells with the ROD-AΔenv vector, an envelope expression vector and pMM310-vpr2 (a derivative of pMM310), a construct encoding β-lactamase (BlaM) fused to the amino terminus of the virion protein vpr2 (BlaM∷vpr2), thereby targeting BlaM to the virion. U87/CD4/X4 cells (2×10^4 cells) or GHOST/X4 cells (1×10^4 cells) in 96-well dishes (clear bottom) were infected with β-lactamase-loaded virus at a moi of 0.5 or higher. After 3 h, the cells were washed twice with PBS and then loaded with 2 μM CCF2/AM/1% probenecid in 50 μl of serum-free, CO_2-independent DMEM for 16–18 h at room temperature. The cells were washed two times with medium and analyzed using a microplate fluorometer (Safire, Tecan, Germany) after excitation at 409 nm. Cleaved substrate was detected as blue fluorescence at 447 nm, and uncleaved substrate was detected as green fluorescence at 520 nm. Fusion of the HIV reporter particles results in delivery of active BlaM into the cytosol; thus, the ratio of blue to green fluorescence is directly correlated with the efficiency of virus–cell fusion (Wyma et al., 2004; Zhou et al., 2004).

CD4 binding and infectivity analysis

For the anti-CD4 antibody inhibition studies on U87/CD4/X4 and GHOST/X4 cells, 3×10^4 cells per well (in a 48 well tray) were pre-treated for 30 min at 37 °C with anti-CD4 antibody at different concentrations (5, 1, 0.2, 0.04, and 0.002 μg of anti-CD4 antibody/ml; Clone RPA-T4, Pharmingen, Germany) before adding equal amounts of particles (5 ng RT-equivalent). The cells were lysed at 2 days post-infection and the renilla luciferase activity (expressed due to infection with ROD-AΔenv-REN derived particles) was measured using the renilla luciferase system (Promega, Germany) and a luminometer (Labsystems, Germany). Duplicate wells were analyzed for each drug concentration in at least three independent experiments. Relative activity (% of control) was calculated by dividing the mean number of relative light units at each anti-CD4 antibody concentration by the mean number of relative light units from cells containing no antibody. For the analysis of particle-associated envelope protein mediated binding to cell-associated CD4 in the absence of any coreceptor, pseudotyped particles containing a mRFP:vpr2

fusion protein were generated. Cotransfection of 293T cells with the ROD-AΔenv vector, an envelope expression vector and pRFP-vpr2, a construct encoding mRFP fused to the amino terminus of the virion protein vpr2 (mRFP::vpr2), thereby targeting mRFP into the virions, resulting in infectious particles that can be monitored due to their red fluorescence. After transfection of 293T cells with the expression plasmid pSG5/CD4-cyt399 (Bedinger et al., 1988; Maddon et al., 1988), which encodes for a truncated CD4 molecule lacking the cytoplasmic tail (CD4-cyt399), the cells were seeded into 96-well dishes at 2×10^4 cells per well and incubated with the different pseudotyped HIV-2 particles (25 ng RT-equivalent) for 1 h at 37 °C/5% CO_2. The binding of viral particles to CD4-cyt399-expressing 293T cells in comparison to 293T cells lacking CD4 was quantitated by excitation of mRFP (584 nm) and recording the emission at 607 nm using a fluorometer (Safire).

Endocytosis of CD4

Basal endocytosis for CD4 expressed on the surface of GHOST/X4 cells and U87/CD4/X4 cells was assayed as described (Schwartz et al., 1996). Briefly, cells were stained at 4 °C for CD4 (clone RPA-T4, BP Pharmingen) in binding medium (BM: RPMI medium, 2% FBS, 20 mM HEPES, pH7.2). Excess antibody was washed away and cells resuspended in cold BM. Cell suspensions were shifted to 37 °C, and, at time points between 0 and 60 min, aliquots were placed on ice. Noninternalized antibody-labeled CD4 were indirectly stained with R-phycoerythrin-conjugated goat anti-mouse antibody (Jackson ImmunoResearch). The endocytosis was assessed by analyzing the decrease of MFI of CD4 staining on viable cells in the course of the kinetic. Percentages of remaining cell surface CD4 at different time points was calculated and plotted over time.

Endosomal particle uptake

To prevent endosome formation, GHOST/X4 cells were nucleofected with expression plasmids encoding for a dynamin-GFP (dynGFP) fusion protein as well as a dominant-negative version of dynamin (dynK44AGFP), respectively (Cao et al., 1998; van der Bliek et al., 1993) according to the manufacturer's protocol (Amaxa, Germany). Cells were seeded into 48-well trays and the next day infected with ROD-AΔenvRFP-derived pseudotyped particles. Forty-eight hours post infection, the fluorescence intensity at 607 nm (mRFP expressing, infected cells) and at 508 nm (nucleofected, GFP-fusion protein expressing cells) was determined. The calculated ratio between these two fluorescence intensities allows a quantification of effective HIV-2 infection dependent on the expression of dominant-negative dynamin versus the expression of wild-type dynamin.

For the inhibition of endosomal acidification, both cell lines were pretreated with NH_4Cl (10 mM) for 30 min at 37 °C before adding equal amounts of infectious virus (ROD-AΔenv-derived particles). The cells were immunostained 2 days post infection and the number of blue cells determined. HIV-2[VSV-G] particles were used to control for complete inhibition of acidification of endosomes.

Stimulation of MAPK family members through particle binding

Prior to stimulation, GHOST/X4 cells were maintained for 48 h in DMEM with 0.1% FCS. Cells were incubated with particle preparations (100 ng RT equivalents) carrying no envelope, Env35, Env42S, 200 ng/ml anisomycin (Sigma) or 10% FCS in the presence or absence of 50 μM UO126 (Cell Signaling Technology, Germany) for 30 min at 37 °C. Cells were washed two times in PBS and lysed in SDS sample buffer. For Western blot analysis, samples were boiled in SDS sample buffer, separated by SDS-10% PAGE, and transferred to a nitrocellulose membrane. Protein detection was performed after incubation with appropriate first and secondary antibodies (Phospho-MAPK family antibody sampler, Cell Signaling Technologies, Germany) by using the Super-Signal Pico detection kit (Pierce, Bonn, Germany) according to the manufacturer's instructions. The detection of 14-3-3γ (loading control) was performed using the polyclonal antibody C-16 (Santa Cruz, Germany) as primary antibody.

Acknowledgments

We wish to thank Drs. Christian Schmitz, Keith Aubin, Áine McKnight (Wohl Virion Centre, London, UK), and Lars Henning for critical discussion during this project, and Isabel Hagmann, Heike Oberwinkler, and Thomas Neumann for tissue culture support.

U87/CD4/X4 cells, GHOST/X4 cells, and HIV-2 serum was provided by the EU programme EVA/MRC centralized facility for AIDS reagents, NIBSC, UK. This work was funded by the Deutsche Forschungsgemeinschaft (DI777). This work counts as partial fulfillment of the PhD requirements for S.R. and P.K. at the University of Heidelberg.

References

Aiken, C., 1997. Pseudotyping human immunodeficiency virus type 1 (HIV-1) by the glycoprotein of vesicular stomatitis virus targets HIV-1 entry to an endocytic pathway and suppresses both the requirement for Nef and the sensitivity to cyclosporin A. J. Virol. 71 (8), 5871–5877.

Alfano, M., Schmidtmayerova, H., Amella, C.A., Pushkarsky, T., Bukrinsky, M., 1999. The B-oligomer of pertussis toxin deactivates CC chemokine receptor 5 and blocks entry of M-tropic HIV-1 strains. J. Exp. Med. 190 (5), 597–605.

Alfano, M., Pushkarsky, T., Poli, G., Bukrinsky, M., 2000. The B-oligomer

of pertussis toxin inhibits human immunodeficiency virus type 1 replication at multiple stages. J. Virol. 74 (18), 8767–8770.
Arthos, J., Rubbert, A., Rabin, R.L., Cicala, C., Machado, E., Wildt, K., Hanbach, M., Steenbeke, T.D., Swofford, R., Farber, J.M., Fauci, A.S., 2000. CCR5 signal transduction in macrophages by human immunodeficiency virus and simian immunodeficiency virus envelopes. J. Virol. 74 (14), 6418–6424.
Bedinger, P., Moriarty, A., von Borstel II, R.C., Donovan, N.J., Steimer, K.S., Littman, D.R., 1988. Internalization of the human immunodeficiency virus does not require the cytoplasmic domain of CD4. Nature 334 (6178), 162–165.
Berger, E.A., Murphy, P.M., Farber, J.M., 1999. Chemokine receptors as HIV-1 coreceptors: roles in viral entry, tropism, and disease. Annu. Rev. Immunol. 17, 657–700.
Best, S., Le Tissier, P., Towers, G., Stoye, J.P., 1996. Positional cloning of the mouse retrovirus restriction gene Fv1. Nature 382 (6594), 826–829.
Boyd, M.T., Simpson, G.R., Cann, A.J., Johnson, M.A., Weiss, R.A., 1993. A single amino acid substitution in the V1 loop of human immunodeficiency virus type 1 gp120 alters cellular tropism. J. Virol. 67 (6), 3649–3652.
Bukrinskaya, A., Brichacek, B., Mann, A., Stevenson, M., 1998. Establishment of a functional human immunodeficiency virus type 1 (HIV-1) reverse transcription complex involves the cytoskeleton. J. Exp. Med. 188 (11), 2113–2125.
Campbell, R.E., Tour, O., Palmer, A.E., Steinbach, P.A., Baird, G.S., Zacharias, D.A., Tsien, R.Y., 2002. A monomeric red fluorescent protein. Proc. Natl. Acad. Sci. U.S.A. 99 (12), 7877–7882.
Cao, H., Garcia, F., McNiven, M.A., 1998. Differential distribution of dynamin isoforms in mammalian cells. Mol. Biol. Cell 9 (9), 2595–2609.
Cavrois, M., De Noronha, C., Greene, W.C., 2002. A sensitive and specific enzyme-based assay detecting HIV-1 virion fusion in primary T lymphocytes. Nat. Biotechnol. 20 (11), 1151–1154.
Chackerian, B., Long, E.M., Luciw, P.A., Overbaugh, J., 1997. Human immunodeficiency virus type 1 coreceptors participate in postentry stages in the virus replication cycle and function in simian immunodeficiency virus infection. J. Virol. 71 (5), 3932–3939.
Cicala, C., Arthos, J., Ruiz, M., Vaccarezza, M., Rubbert, A., Riva, A., Wildt, K., Cohen, O., Fauci, A.S., 1999. Induction of phosphorylation and intracellular association of CC chemokine receptor 5 and focal adhesion kinase in primary human CD4+ T cells by macrophage-tropic HIV envelope. J. Immunol. 163 (1), 420–426.
Clapham, P.R., McKnight, A., 2002. Cell surface receptors, virus entry and tropism of primate lentiviruses. J. Gen. Virol. 83 (Pt. 8), 1809–1829.
Dejucq, N., Simmons, G., Clapham, P.R., 1999. Expanded tropism of primary human immunodeficiency virus type 1 R5 strains to CD4 (+) T-cell lines determined by the capacity to exploit low concentrations of CCR5. J. Virol. 73 (9), 7842–7847.
Dvorin, J.D., Malim, M.H., 2003. Intracellular trafficking of HIV-1 cores: journey to the center of the cell. Curr. Top. Microbiol. Immunol. 281, 179–208.
Eckert, D.M., Kim, P.S., 2001. Mechanisms of viral membrane fusion and its inhibition. Annu. Rev. Biochem. 70, 777–810.
Fackler, O.T., Peterlin, B.M., 2000. Endocytic entry of HIV-1. Curr. Biol. 10 (16), 1005–1008.
Greene, W.C., Peterlin, B.M., 2002. Charting HIV's remarkable voyage through the cell: Basic science as a passport to future therapy. Nat. Med. 8 (7), 673–680.
Hatziioannou, T., Perez-Caballero, D., Yang, A., Cowan, S., Bieniasz, P.D., 2004. Retrovirus resistance factors Ref1 and Lv1 are species-specific variants of TRIM5α . Proc. Natl. Acad. Sci. U.S.A. 101 (29), 10774–10779.
Keckesova, Z., Ylinen, L.M., Towers, G.J., 2004. The human and African green monkey TRIM5a genes encode Ref1 and Lv1 retroviral restriction factor activities. Proc. Natl. Acad. Sci. U.S.A. 101 (29), 10780–10785.
Kinet, S., Bernard, F., Mongellaz, C., Perreau, M., Goldman, F.D., Taylor, N., 2002. gp120-mediated induction of the MAPK cascade is dependent on the activation state of CD4 (+) lymphocytes. Blood 100 (7), 2546–2553.
Kizhatil, K., Albritton, L.M., 1997. Requirements for different components of the host cell cytoskeleton distinguish ecotropic murine leukemia virus entry via endocytosis from entry via surface fusion. J. Virol. 71 (10), 7145–7156.
Lineberger, J.E., Danzeisen, R., Hazuda, D.J., Simon, A.J., Miller, M.D., 2002. Altering expression levels of human immunodeficiency virus type 1 gp120–gp41 affects efficiency but not kinetics of cell–cell fusion. J. Virol. 76 (7), 3522–3533.
Liu, Q.H., Williams, D.A., McManus, C., Baribaud, F., Doms, R.W., Schols, D., De Clercq, E., Kotlikoff, M.I., Collman, R.G., Freedman, B.D., 2000. HIV-1 gp120 and chemokines activate ion channels in primary macrophages through CCR5 and CXCR4 stimulation. Proc. Natl. Acad. Sci. U.S.A. 97 (9), 4832–4837.
Maddon, P.J., McDougal, J.S., Clapham, P.R., Dalgleish, A.G., Jamal, S., Weiss, R.A., Axel, R., 1988. HIV infection does not require endocytosis of its receptor, CD4. Cell 54 (6), 865–874.
Marechal, V., Prevost, M.C., Petit, C., Perret, E., Heard, J.M., Schwartz, O., 2001. Human immunodeficiency virus type 1 entry into macrophages mediated by macropinocytosis. J. Virol. 75 (22), 11166–11177.
McDonald, D., Vodicka, M.A., Lucero, G., Svitkina, T.M., Borisy, G.G., Emerman, M., Hope, T.J., 2002. Visualization of the intracellular behavior of HIV in living cells. J. Cell Biol. 159 (3), 441–452.
McKnight, A., Griffiths, D.J., Dittmar, M., Clapham, P., Thomas, E., 2001. Characterization of a late entry event in the replication cycle of human immunodeficiency virus type 2. J. Virol. 75 (15), 6914–6922.
Mori, K., Ringler, D.J., Desrosiers, R.C., 1993. Restricted replication of simian immunodeficiency virus strain 239 in macrophages is determined by env but is not due to restricted entry. J. Virol. 67 (5), 2807–2814.
Naif, H.M., Li, S., Alali, M., Sloane, A., Wu, L., Kelly, M., Lynch, G., Lloyd, A., Cunningham, A.L., 1998. CCR5 expression correlates with susceptibility of maturing monocytes to human immunodeficiency virus type 1 infection. J. Virol. 72 (1), 830–836.
Otto, C., Puffer, B.A., Pohlmann, S., Doms, R.W., Kirchhoff, F., 2003. Mutations in the C3 region of human and simian immunodeficiency virus envelope have differential effects on viral infectivity, replication, and CD4-dependency. Virology 315 (2), 292–302.
Pedroza-Martins, L., Gurney, K.B., Torbett, B.E., Uittenbogaart, C.H., 1998. Differential tropism and replication kinetics of human immunodeficiency virus type 1 isolates in thymocytes: coreceptor expression allows viral entry, but productive infection of distinct subsets is determined at the postentry level. J. Virol. 72 (12), 9441–9452.
Pelchen-Matthews, A., Clapham, P., Marsh, M., 1995. Role of CD4 endocytosis in human immunodeficiency virus infection. J. Virol. 69 (12), 8164–8168.
Perron, M.J., Stremlau, M., Song, B., Ulm, W., Mulligan, R.C., Sodroski, J., 2004. TRIM5α mediates the postentry block to N-tropic murine leukemia viruses in human cells. Proc. Natl. Acad. Sci. U.S.A. 27, 27.
Platt, E.J., Wehrly, K., Kuhmann, S.E., Chesebro, B., Kabat, D., 1998. Effects of CCR5 and CD4 cell surface concentrations on infections by macrophagetropic isolates of human immunodeficiency virus type 1. J. Virol. 72 (4), 2855–2864.
Pontow, S.E., Heyden, N.V., Wei, S., Ratner, L., 2004. Actin cytoskeletal reorganizations and coreceptor-mediated activation of rac during human immunodeficiency virus-induced cell fusion. J. Virol. 78 (13), 7138–7147.
Popik, W., Pitha, P.M., 2000a. Exploitation of cellular signaling by HIV-1: unwelcome guests with master keys that signal their entry. Virology 276 (1), 1–6.
Popik, W., Pitha, P.M., 2000b. Inhibition of CD3/CD28-mediated activation of the MEK/ERK signaling pathway represses replication of X4 but not R5 human immunodeficiency virus type 1 in peripheral blood CD4 (+) T lymphocytes. J. Virol. 74 (6), 2558–2566.
Reeves, J.D., Miamidian, J.L., Biscone, M.J., Lee, F.H., Ahmad, N., Pierson, T.C., Doms, R.W., 2004. Impact of mutations in the coreceptor

binding site on human immunodeficiency virus type 1 fusion, infection, and entry inhibitor sensitivity. J. Virol. 78 (10), 5476–5485.

Schaeffer, E., Soros, V.B., Greene, W.C., 2004. Compensatory link between fusion and endocytosis of human immunodeficiency virus type 1 in human CD4 T lymphocytes. J. Virol. 78 (3), 1375–1383.

Schambach, A., Wodrich, H., Hildinger, M., Bohne, J., Krausslich, H.G., Baum, C., 2000. Context dependence of different modules for posttranscriptional enhancement of gene expression from retroviral vectors. Mol. Ther. 2 (5), 435–445.

Schmidtmayerova, H., Alfano, M., Nuovo, G., Bukrinsky, M., 1998. Human immunodeficiency virus type 1 T-lymphotropic strains enter macrophages via a CD4- and CXCR4-mediated pathway: replication is restricted at a postentry level. J. Virol. 72 (6), 4633–4642.

Schmitz, C., Marchant, D., Neil, S.J., Aubin, K., Reuter, S., Dittmar, M.T., McKnight, A., Kizhatil, K., Albritton, L.M., 2004. Lv2, a novel postentry restriction, is mediated by both capsid and envelope. J. Virol. 78 (4), 2006–2016.

Schwartz, O., Marechal, V., Le Gall, S., Lemonnier, F., Heard, J.M., 1996. Endocytosis of major histocompatibility complex class I molecules is induced by the HIV-1 Nef protein. Nat. Med. 2 (3), 338–342.

Stoye, J.P., 2002. An intracellular block to primate lentivirus replication. Proc. Natl. Acad. Sci. U.S.A. 99 (18), 11549–11551.

Stremlau, M., Owens, C.M., Perron, M.J., Kiessling, M., Autissier, P., Sodroski, J., 2004. The cytoplasmic body component TRIM5a restricts HIV-1 infection in Old World monkeys. Nature 427 (6977), 848–853.

Towers, G., Bock, M., Martin, S., Takeuchi, Y., Stoye, J.P., Danos, O., 2000. A conserved mechanism of retrovirus restriction in mammals. Proc. Natl. Acad. Sci. U.S.A. 97 (22), 12295–12299.

van der Bliek, A.M., Redelmeier, T.E., Damke, H., Tisdale, E.J., Meyerowitz, E.M., Schmid, S.L., 1993. Mutations in human dynamin block an intermediate stage in coated vesicle formation. J. Cell Biol. 122 (3), 553–563.

Verani, A., Pesenti, E., Polo, S., Tresoldi, E., Scarlatti, G., Lusso, P., Siccardi, A.G., Vercelli, D., 1998. CXCR4 is a functional coreceptor for infection of human macrophages by CXCR4-dependent primary HIV-1 isolates. J. Immunol. 161 (5), 2084–2088.

Wyma, D.J., Jiang, J., Shi, J., Zhou, J., Lineberger, J.E., Miller, M.D., Aiken, C., 2004. Coupling of human immunodeficiency virus type 1 fusion to virion maturation: a novel role of the gp41 cytoplasmic tail. J. Virol. 78 (7), 3429–3435.

Yang, X., Gabuzda, D., 1999. Regulation of human immunodeficiency virus type 1 infectivity by the ERK mitogen-activated protein kinase signaling pathway. J. Virol. 73 (4), 3460–3466.

Yap, M.W., Nisole, S., Lynch, C., Stoye, J.P., 2004. Trim5α protein restricts both HIV-1 and murine leukemia virus. Proc. Natl. Acad. Sci. U.S.A. 101 (29), 10786–10791.

Zhou, J., Yuan, X., Dismuke, D., Forshey, B.M., Lundquist, C., Lee, K.H., Aiken, C., Chen, C.H., 2004. Small-molecule inhibition of human immunodeficiency virus type 1 replication by specific targeting of the final step of virion maturation. J. Virol. 78 (2), 922–929.